electronics

MDPI

Communication

Effects of Gamma Irradiation on Switching Characteristics of SiC MOSFET Power Devices of Different Structures

Lei Shu [1,2,3], Huai-Lin Liao [1], Zi-Yuan Wu [4], Xing-Yu Fang [2,3], Shi-Wei Liang [4], Tong-De Li [2,3], Liang Wang [2,3], Jun Wang [4] and Yuan-Fu Zhao [2,3,*]

1 School of Integrated Circuit, Peking University, Beijing 100871, China; 18001350960@163.com (L.S.)
2 Beijing Microelectronics Technology Institute, Beijing 100076, China
3 Laboratory of Science and Technology on Radiation Hardened Integrated Circuits, China Aerospace Science and Technology Corporation (CASC) Fengtai, Beijing 100076, China
4 College of Electrical and Information Engineering, Hunan University, Changsha 410082, China
* Correspondence: zhaoyf@vip.163.com

Abstract: The switching characteristics of silicon carbide (SiC) metal-oxide-semiconductor field-effect transistor (MOSFET) power devices of different structures were experimented after exposure to a gamma irradiation environment. The experimental results for on-state were studied. The comparisons are shown for SiC MOSFET power devices with planar, trench and double trench structures tested for total ionizing dose (TID). A higher degradation of the switching characteristics was observed for the double trench structure. The physical mechanisms for these switching characteristics variations were analyzed. In addition, they were confirmed by technology computer-aided design (TCAD) simulation.

Keywords: SiC MOSFET; TID; switching characteristic; TCAD simulations

check for updates

Citation: Shu, L.; Liao, H.-L.; Wu, Z.-Y.; Fang, X.-Y.; Liang, S.-W.; Li, T.-D.; Wang, L.; Wang, J.; Zhao, Y.-F. Effects of Gamma Irradiation on Switching Characteristics of SiC MOSFET Power Devices of Different Structures. *Electronics* **2023**, *12*, 2194. https://doi.org/10.3390/electronics12102194

Received: 3 April 2023
Revised: 16 April 2023
Accepted: 20 April 2023
Published: 11 May 2023

Copyright: © 2023 by the authors. Licensee MDPI, Basel, Switzerland. This article is an open access article distributed under the terms and conditions of the Creative Commons Attribution (CC BY) license (https://creativecommons.org/licenses/by/4.0/).

1. Introduction

Silicon carbide metal-oxide-semiconductor field-effect transistor (SiC MOSFET) power devices have a higher critical electric field and higher electron velocity than silicon, making them one the most promising power switches in space power systems [1–3]. However, SiC MOSFETs will be affected when working in space by TID due to radiation-induced trapped charges in the gate oxide (GOX), which in turn leads to their static and dynamic characteristic variations [4]. Currently, most of the published literature focuses on the TID effect on the static characteristics of SiC MOSFET power devices, and fewer published papers focus on the TID effects on the dynamic characteristics of SiC MOSFET power devices [5–9]. Only few papers have studied the TID effects on the dynamic characteristics of SiC MOSFET power devices, including switching characteristics [9,10]. These published results have only studied the experimental phenomena of the TID effects on the switching characteristics of the SiC MOSFET, without investigating the failure mechanisms of the switching characteristics in detail.

This paper investigates TID effects on the switching characteristics of 1200 V commercial SiC MOSFET power devices, and the failure mechanisms, through experiment and TCAD simulation. The details of the SiC MOSFET power devices under experimental processes are introduced in Section 2. The experimental results are shown in Section 3. The analysis and TCAD simulation are shown in Section 4, followed by conclusions in Section 5.

2. Device Description and Experimental Setup

Figure 1 shows the cross-sectional views of the studied SiC MOSFET power devices of different structures. Figure 1a–c show the schematic cross-sectional view of planar structure, trench structure and double trench structure, respectively. The studied devices are commercial SiC MOSFETs from CREE (C3M0075120D), Infineon (IMW120R090M1H)

and Rohm (SCT3080KR) Corporation, respectively. The rated voltage of these devices is 1200 V.

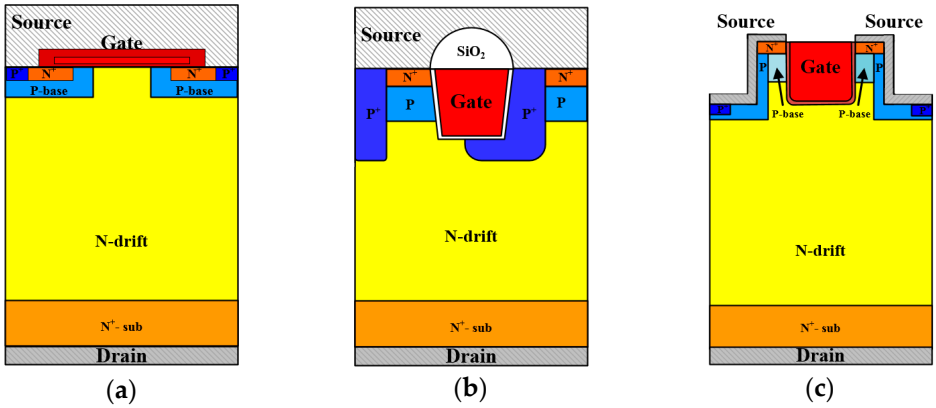


Figure 1. Schematic cross-sectional view of (**a**) planar structure, (**b**) trench structure and (**c**) double trench structure of SiC MOSFET power devices.

The TID experiment was performed at the National Institute of Metrology, China. Co-60 gamma rays were sourced at a dose rate of 50 rad (Si)/s. The device samples were irradiated under on-bias condition. The on-bias condition was VGS = 15 V and VDS = 0 V. The planar devices were irradiated to a total dose of 500 krad(Si) and the trench and double trench devices were irradiated to a total dose of 100 krad(Si). The threshold voltage (VTH) of CREE and Rohm is defined as the value of the gate-voltage at the drain current of 5 mA [11,12] and the VTH of Infineon is defined as the drain current of 3.7 mA [13].

The studied switching characteristics, including turn-on delay time (tdon), rise time (tr), turn-off delay time (tdoff) and fall time (tf), etc., are extracted through a double pulse test (DPT) platform according to the datasheets [11–13]. The switching characteristics test platform is shown in Figure 2. Figure 2a shows the schematic of the DPT circuit. Figure 2b is a picture of the DPT platform. Figure 2c shows the theoretical waveforms of the DPT.

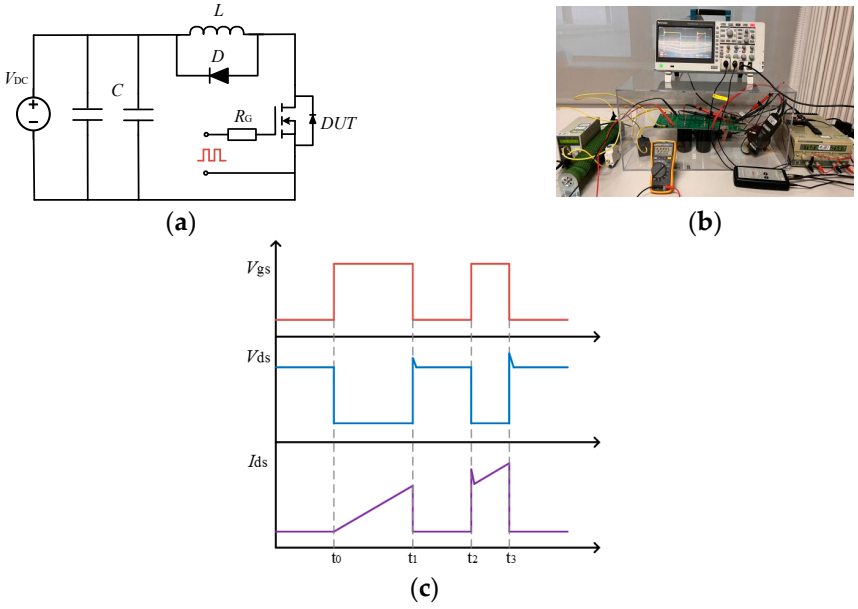


Figure 2. Switching characteristics test platform. (**a**) The schematic of double pulse test circuit, (**b**) a picture of the double pulse test platform and (**c**) double pulse theoretical waveforms.

3. Experimental Results

3.1. Measured Threshold Characteristics after Irradiation

The measured transfer characteristic curves with three different architectures at different dose levels are shown in Figure 3. The characteristic curves of planar structure, trench structure and double trench structure are shown in Figure 3a–c, respectively. All of the plots present transfer and breakdown characteristics before irradiation as solid lines and after irradiation as dash-dotted lines. The irradiated devices exhibit different transfer characteristics degradation behavior under on-bias.

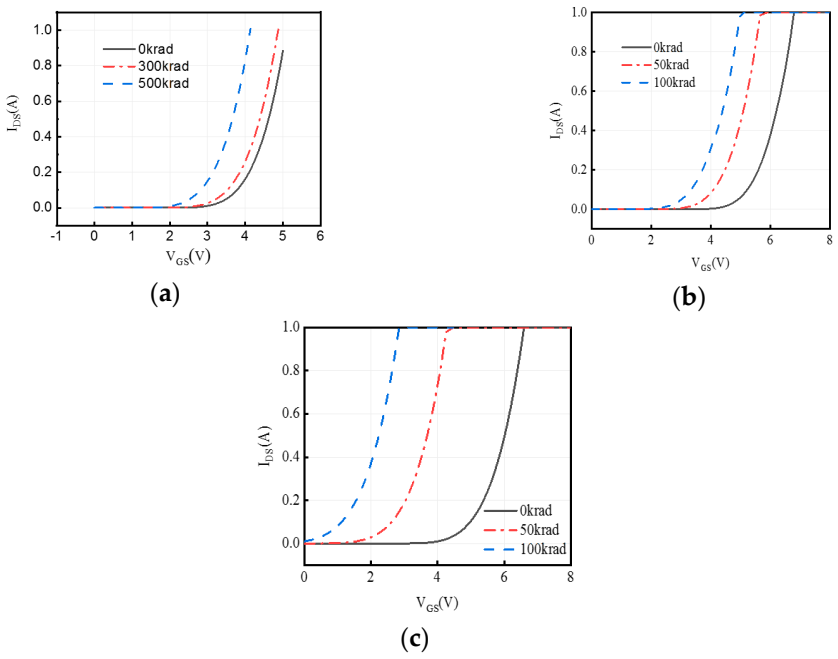


Figure 3. Measured transfer characteristic curves of SiC MOSFET power devices before and after irradiation. (**a**) Planar structure, (**b**) trench structure and (**c**) double trench structure.

For the transfer characteristic curves of planar structure, threshold voltage (VTH) decreases steadily to about 2.5 V from its rated voltage of 3.5 V for non-irradiated devices as the dose accumulates to 500 krad(Si). From Figure 3b,c, it can be seen that the VTH of trench structure and double trench structure decrease steadily to about 2.5 V and 0.2 V as the dose accumulates to 100 krad(Si), respectively. Their rated voltage is, in all, about 4.5 V for non-irradiated devices.

The radiation-induced VTH degradation rate for the SiC MOSFET power devices of these three architectures is about 28.6%, 44.4% and 95.6%, respectively. By comparing the VTH degradation rate of the three architectures, it can be shown that radiation produces the most trap charges on the GOX of the double trench structure. The planar MOSFETs from CREE have a higher tolerance to TID with respect to the trench and double trench devices.

3.2. Measured Turn-On/Off Time Characteristics after Irradiation

Figures 4 and 5 show the turn-on and turn-off times of the three architectures at different dose levels, respectively. The turn-on time (ton) and turn-off time (toff) are extracted by DPT platform. The extracted turn-on and turn-off time include turn-on delay time (tdon), rise time (tr), turn-off delay time (tdoff) and fall time (tf), respectively. The extracted tdon and tr of the planar structure before and after irradiation are shown in Figure 4a. Figure 4b,c show the extracted tdon and tr of the trench and double trench structures before and after irradiation, respectively. From Figure 4a, it can be seen that the tdon and tr of the planar structure decrease by about 0.6 ns and 1.8 ns at TID = 500 krad(Si), respectively. The influence of radiation on the tdon and tr of the planar structure is

negligible. For trench structure and double trench structure, their tdon and tr reduce by about 1 ns and 9.3 ns, 7.8 ns and 18 ns at TID = 100 krad(Si), respectively.

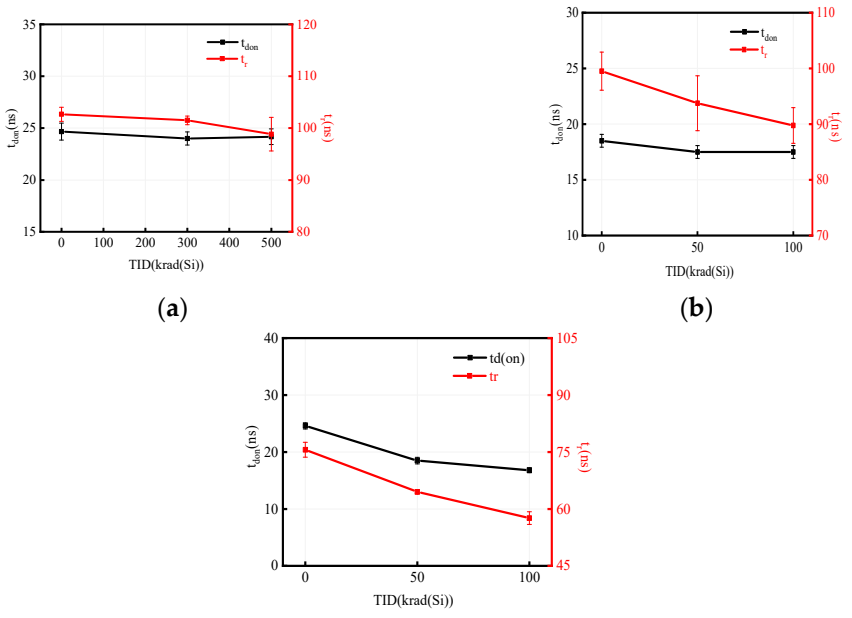


Figure 4. Comparison of measured turn-on delay time and rise time characteristics of SiC MOSFETs of different structures with TID. (**a**) Planar structure, (**b**) trench structure and (**c**) double trench structure.

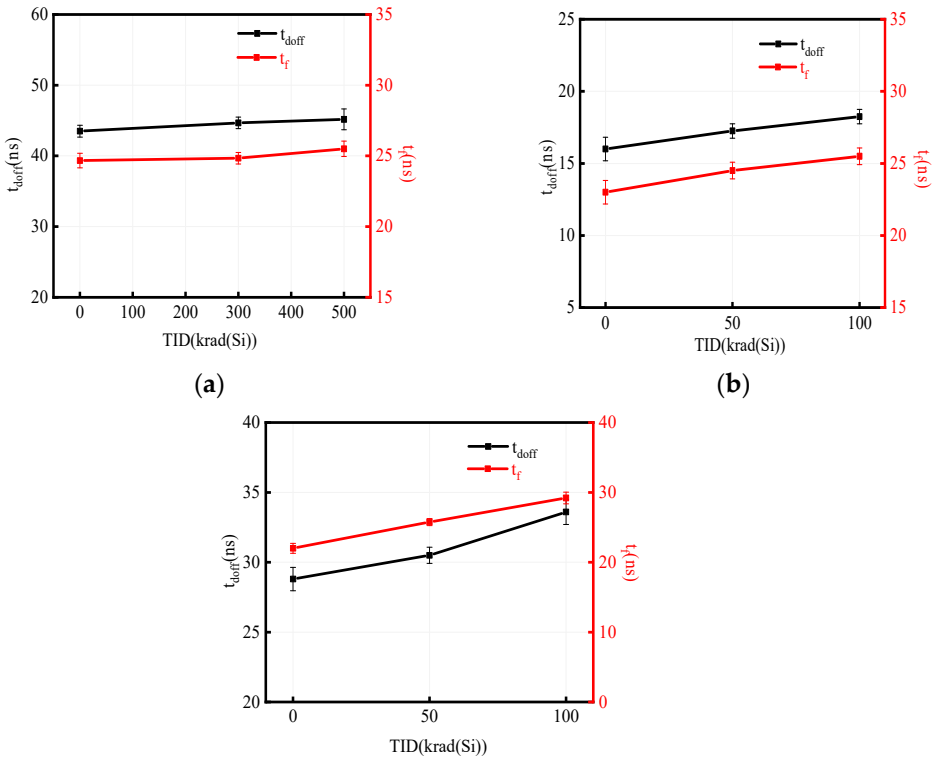


Figure 5. Comparison of measured turn-off delay time and fall time characteristics of SiC MOSFETs of different structures with TID. (**a**) Planar structure, (**b**) trench structure and (**c**) double trench structure.

Figure 4a–c show the extracted tdoff and tf of the planar, trench and double trench structures before and after irradiation, respectively. For the planar structure, the extracted

tdoff and tf increase by about 1.7 ns and 0.9 ns, respectively. There was very little variation. For trench structure and double trench structure, their tdoff and tf increase by about 2.25 ns and 2.5 ns, 4.8 ns and 7.2 ns with a dose of up to 100 krad(Si), respectively. By comparing the turn-on and turn-off time of the three architectures, we observed that planar structure is insensitive to TID and double trench structure is greatly influenced by TID.

3.3. Measured Turn-On/Off Energy Loss Characteristics after Irradiation

The turn-on energy loss (Eon) and turn-off energy loss (Eoff) of the three architectures at different dose levels are shown in Figures 6 and 7, respectively. The Eon and Eoff are also extracted by DPT platform. The extracted Eon of the planar structure is shown in Figure 6a. From Figure 6a, it can be seen that as the dose accumulates to 500 krad(Si), Eon decreases to about 368.5 mJ from its rated Eon of about 402.6 mJ for non-irradiated devices. The Eon decrease rate is about 8.5% at TID = 500 krad(Si). From Figure 6b,c, it can be seen that Eon of the trench structure and double trench structure decrease by about 72.3 mJ and 82 mJ with dose accumulation up to 100 krad(Si), respectively. Their Eon decrease rates are about 18.6% and 45.5%, respectively.

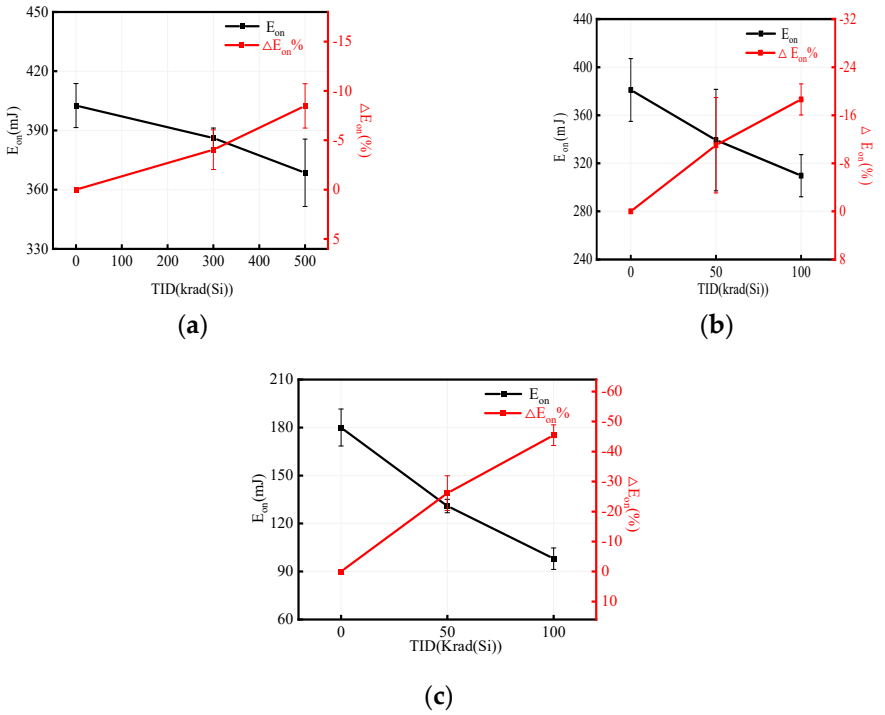


Figure 6. Comparison of measured Eon and Eon variation rate of different structures before and after irradiation. (**a**) Planar structure, (**b**) trench structure and (**c**) double trench structure.

Figure 7a–c show the extracted Eoff of the planar, trench and double trench structures before and after irradiation, respectively. From Figure 7a, we observe that the Eoff of the planar structure decreases by 0.7 mJ with dose accumulation up to 300 krad(Si). However, as the dose accumulated to 500 krad(Si), the Eoff began to increase by 0.6 mJ at TID = 500 krad(Si) compared to the device for non-irradiated. By Figure 7a, it can be seen that the Eoff of the planar structure is influenced by TID and can be ignored.

The Eoff of the trench and double trench structures consistently increases with doses up to 100 krad(Si), as shown in Figure 7b,c. As the dose accumulates to 100 krad(Si), the Eoff of the trench and double trench structures increases by about 11 mJ and 38 mJ, respectively. Their Eoff increase rates are 8.85% and 32.9%, respectively.

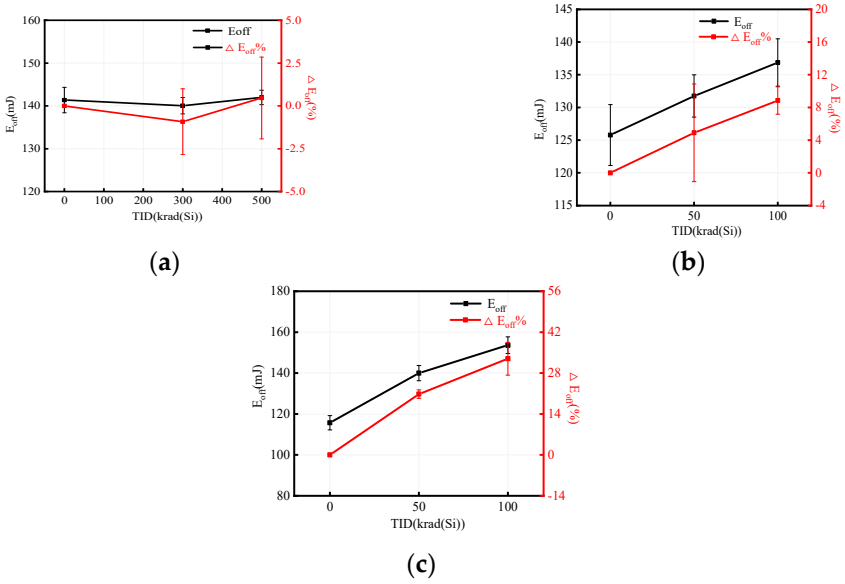


Figure 7. Comparison of measured Eoff and Eoff variation rates of different structures before and after irradiation. (**a**) Planar structure, (**b**) trench structure and (**c**) double trench structure.

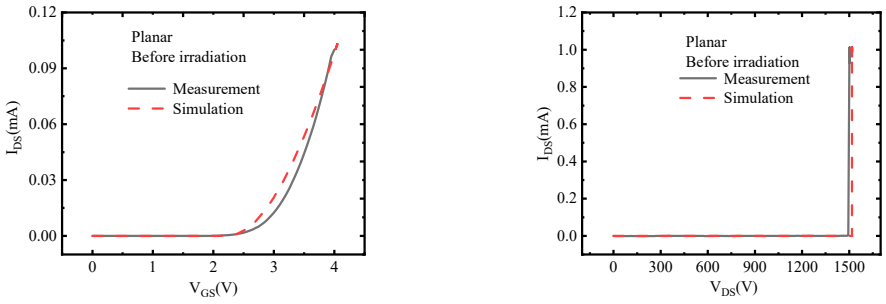
4. Analysis and Simulations

TID caused oxide-trapped charges and interface charges in the gate oxide (GOX) [14]. In contrast to the interface charges, TID caused substantial oxide-trapped charges in GOX. The trapped positive charge is the main cause of the threshold voltage shifting negatively. Through experimental studies, tdon and tr are shown to be proportional to VTH at different dose levels. However, tdoff and tf are inversely proportional to VTH at different dose levels. Since VTH decreases with the increasing oxide-trapped charges on GOX, the tdon and tr reduction and tdoff and tf increase with dose accumulated are due to the trapped charge generated by radiation induced on GOX. Comparing the GOX structures of the planar, trench and double trench SiC MOSFETs (seen from Figure 1), the double trench SiC MOSFET has three GOX interfaces with the largest number, while the planar SiC MOSFET has only one GOX interface with the smallest number. Thus, at the same dose level, the most oxide-trapped charges are generated on the double trench structure and the least on the planar structure. Based on the above analysis, radiation-induced oxide-trapped charges are the main cause of the tdon, tr, tdoff and tf change. The Eon and Eoff are proportional to turn-on and turn-off time, drain voltage and drain current, respectively [2]. Turn-on and turn-off time are equal to tdon plus tr and tdoff plus tf, respectively. Therefore, the main reason for the Eon decrease and Eoff increase as accumulated dose increases is also trapped charges induced by radiation on GOX.

To further research these TID effects, 2D TCAD simulation models were developed. We chose SiC MOSFETs of planar structure as examples for simulation studies. The simulation model is developed based on the planar structure (similar to Figure 1a). The parameters were calibrated by fitting simulation results to measurement data for non-irradiated SiC MOSFETs. Figure 8a,b show the transfer characteristics and breakdown characteristics of the measured device and the simulation model, respectively. From Figure 8, we can see that the simulation results fit relatively well with the test results. To imitate the TID effect, charges are placed inside the GOX, 5 nm from the SiC-SiO2.

To simulate the TID irradiation, positive charge density expressed as Not are put in the GOX of the device models. Figure 9 shows the simulation results for turn-on and turn-off transients of SiC MOSFETs before and after irradiation with Not_GOX = $2 \times 10^{12}/cm^2$ and $2.5 \times 10^{12}/cm^2$. The simulated drain voltage waveforms, gate voltage waveforms and drain current waveforms before and after irradiation are shown in Figure 9a–c, respectively. From Figure 9a, it can be seen that the drain voltage waveforms of the SiC MOSFETs shift negatively at the turn-on moment after irradiation, while the waveforms shift positively at

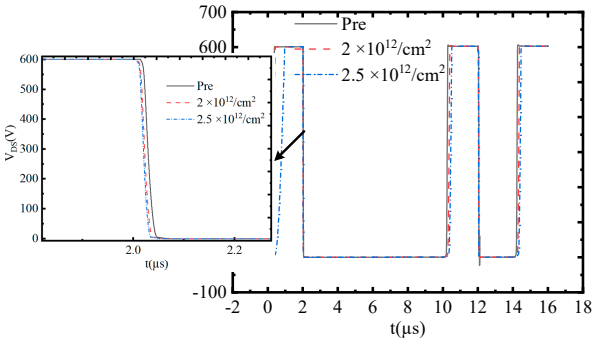
the turn-off moment. After irradiation, the gate voltage waveforms of the SiC MOSFETs shift positively at the turn-on and turn-off moments. In addition, the drain current of the SiC MOSFETs increases after irradiation.



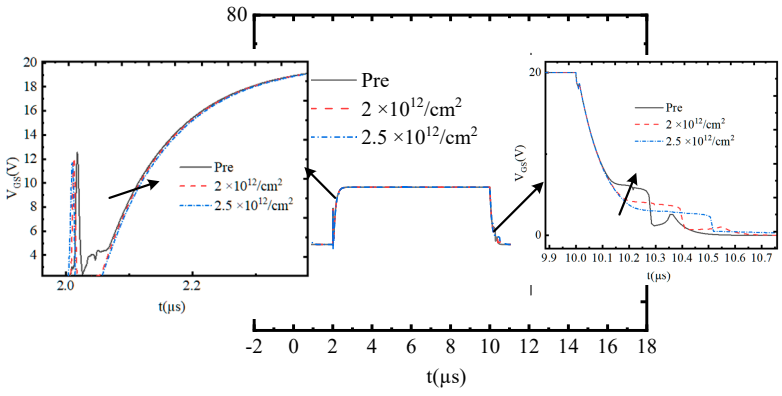
(**a**) (**b**)

Figure 8. Simulation and measured non-irradiated (**a**) threshold characteristics and (**b**) breakdown characteristics curves for SiC MOSFET power devices with planar structure.

From the datasheet of 1200 V SiC MOSFETs as shown in Figure 10, the relationships between tdon, tr, tdoff and tf, and the drain voltage waveforms and gate voltage waveforms [11] can be seen. Tdon equals the time corresponding to 90% of VDS minus the time corresponding to 10% of VGS. Tdoff equals the time corresponding to 10% of VDS minus the time corresponding to 90% of VGS. Combining the relationship of tdon and tdoff with VDS and VGS, the simulated results of drain and gate voltage waveforms (shown in Figure 9a,b) show that the trapped charges generated by radiation are the main reason for tdon decreases and tdoff increases.



(**a**)



(**b**)

Figure 9. *Cont.*

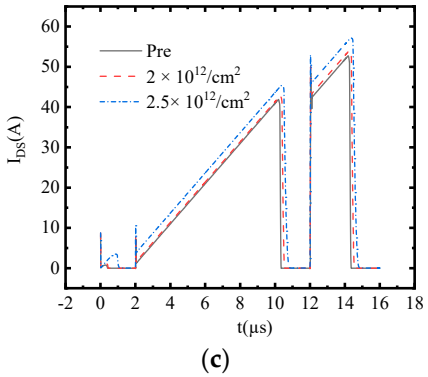


Figure 9. Comparison of simulated turn−on and turn−off transients of SiC MOSFETs with planar structure before and after irradiation with Not_GOX = $2 \times 10^{12}/cm^2$ and $2.5 \times 10^{12}/cm^2$. (**a**) Drain voltage waveforms, (**b**) gate voltage waveforms and (**c**) drain current waveforms.

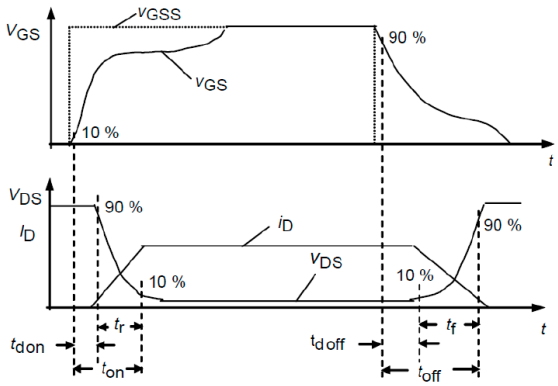


Figure 10. Switching times definition.

For tr and tf, Figure 10 shows that tr and tf equal the time corresponding to 10% of VDS minus 90% of VDS and 90% of VDS minus 10% of VDS, respectively. From the simulated results in Figure 9a, it can be calculated that the tr value before radiation is 15 ns and the tr values are 14 ns and 12.3 ns at Not_GOX = $2 \times 10^{12}/cm^2$ and $2.5 \times 10^{12}/cm^2$, respectively. By the same calculation, the tf before radiation is 40 ns and the tf values are 78 ns and 91.8 ns at Not_GOX = $2 \times 10^{12}/cm^2$ and $2.5 \times 10^{12}/cm^2$, respectively. Through the calculation results, it can be found that the reason for tr decreases and tf increases with dose accumulation are also caused by the trapped charges generated by radiation induced on GOX. The tr values are 14 ns and 12.3 ns at Not_GOX = $2 \times 10^{12}/cm^2$ and $2.5 \times 10^{12}/cm^2$, respectively.

Eon and Eoff are equal to the drain voltage multiplied with the drain current and then integrated with the turn-on time and turn-off time, respectively. The simulated results in Figure 9 show that radiation induced on GOX is also the main cause of the Eon and Eoff variations.

Comparing the experimental results from Figure 3, it can be seen that radiation generated the most trapped charges on GOX in the double trench SiC MOSFET and the least in the planar SiC MOSFET. The degradation mechanisms of the switching characteristics of the trench and double trench SiC MOSFET power devices are similar to that of the planar SiC MOSFET power devices, where the radiation induced oxide-trapped charges on GOX.

5. Conclusions

This paper experimentally measured the turn-on time, turn-off time, turn-on energy loss and turn-off energy loss variations for 1200 V commercial SiC MOSFET power devices with three architectures induced by TID. The switching characteristic variations of these three architectures behave differently for these devices after irradiation. Compared with

trench and double trench structures, the switching characteristics of the planar structure are almost unchanged after irradiation. These behaviors can be attributed to radiation-induced trapped charges in the GOX. These results provide some insights for the application and design of high-voltage SiC MOSFETs in space radiation environments.

Author Contributions: Conceptualization, L.S.; methodology, S.-W.L.; software, X.-Y.F.; validation, T.-D.L. and L.W.; formal analysis, L.S.; investigation, L.S.; resources, J.W.; data curation, Z.-Y.W.; writing—original draft preparation, L.S.; writing—review and editing, Y.-F.Z.; visualization, Z.-Y.W.; supervision, H.-L.L.; project administration, Y.-F.Z.; funding acquisition, L.S. All authors have read and agreed to the published version of the manuscript.

Funding: This work was supported in part by the National Natural Science Foundation of China under Grant 62204019 and 52207199, in part by the science and technology innovation Program of Hunan Province under Grant 2021RC2044.

Institutional Review Board Statement: Not applicable.

Informed Consent Statement: Not applicable.

Data Availability Statement: Not applicable.

Conflicts of Interest: The authors declare no conflict of interest.

References

1. Ball, D.R.; Galloway, K.F.; Johnson, R.A.; Alles, M.L.; Sternberg, A.L.; Witulski, A.F.; Reed, R.A.; Schrimpf, R.D.; Hutson, J.M.; Lauenstein, J.-M. Effects of Breakdown Voltage on Single Event Burnout Tolerance of High-Voltage SiC Power MOSFETs. *IEEE Trans. Nucl. Sci.* **2021**, *68*, 1430–1435. [CrossRef]
2. Na, J.; Kim, K. A Novel 4H-SiC Double Trench MOSFET with Built-In MOS Channel Diode for Improved Switching Performance. *Electronics* **2013**, *12*, 92. [CrossRef]
3. Yabin, S.; Wan, X.; Liu, Z.; Jin, H.; Yan, J.; Li, X.; Shi, Y. Investigation of total ionizing dose effects in 4H–SiC power MOSFET under gamma ray radiation. *Radiat. Phys. Chem.* **2022**, *197*, 110219.
4. Luo, Z.; Chen, T.; Cressler, J.D.; Sheridan, D.C.; Williams, J.R.; Reed, R.A.; Marshall, P.W. Impact of proton irradiation on the static and dynamic characteristics of high-voltage 4H-SiC JBS switching diodes. *IEEE Trans. Nucl. Sci.* **2003**, *50*, 1821–1826.
5. Hazdra, P.; Popelka, S. Displacement damage and total ionization dose effects on 4H-SiC power devices. *IET Power Electron.* **2019**, *12*, 3910–3918. [CrossRef]
6. Hu, D.; Zhang, J.; Jia, Y.; Wu, Y.; Peng, L.; Tang, Y. Impact of Different Gate Biases on Irradiation and Annealing Responses of SiC MOSFETs. *IEEE Trans. Electron Devices* **2018**, *65*, 3719–3724. [CrossRef]
7. Krishnamurthy, S.; Kannan, R.; Kiong, C.C.; Ibrahim, T.B.; Abdullah, Y. Impact of Gamma-ray Irradiation on Dynamic Characteristics of Si and SiC Power MOSFETs. *Int. J. Electr. Comput. Eng. Sci.* **2019**, *9*, 1453–1460.
8. Akturk, A.; McGarrity, J.M.; Potbhare, S.; Goldsman, N. Radiation Effects in Commercial 1200 V 24 A Silicon Carbide Power *MOSFETs*. *IEEE Trans. Nucl. Sci.* **2012**, *59*, 3258–3264. [CrossRef]
9. Feng, H.; Yang, S.; Liang, X.; Zhang, D.; Pu, X.; Cui, X.; Wang, H.; Sun, J.; Yu, X.; Guo, Q. Radiation Effects and Mechanisms on Switching Characteristics of Silicon Carbide Power MOSFETs. *J. Nanoelectron. Optoelectron.* **2021**, *16*, 1423–1429. [CrossRef]
10. Godignon, P.; Massetti, S.; Jordà, X.; Soler, V.; Moreno, J.; Lopez, D.; Maset, E. SiC Power Switches Evaluation for Space Applications Requirements. *Mater. Sci. Forum* **2016**, *858*, 852–855. [CrossRef]
11. Available online: https://www.alldatasheet.com/view.jsp?Searchword=C3M0075120D&sField=4 (accessed on 1 February 2019).
12. Available online: https://www.alldatasheet.com/view.jsp?Searchword=SCT3080KR&sField=4 (accessed on 1 July 2019).
13. Available online: https://www.infineon.com/cms/cn/product/power/mosfet/silicon-carbide/discretes/imw120r090m1h/ (accessed on 1 December 2020).
14. Schwank, J.R.; Shaneyfelt, M.R.; Fleetwood, D.M.; Felix, J.A.; Dodd, P.E.; Paillet, P.; Ferlet-Cavrois, V. Radiation Effects in MOS Oxides. *IEEE Trans. Nucl. Sci.* **2008**, *55*, 1833–1853. [CrossRef]

Disclaimer/Publisher's Note: The statements, opinions and data contained in all publications are solely those of the individual author(s) and contributor(s) and not of MDPI and/or the editor(s). MDPI and/or the editor(s) disclaim responsibility for any injury to people or property resulting from any ideas, methods, instructions or products referred to in the content.